Mechanics of Blood Flow in Capillaries

Timothy W. SECOMB *

* Corresponding author: Tel.: 520-626-4513; Fax: 520-626-3376; Email: secomb@u.arizona.edu
Departments of Physiology and Mathematics, University of Arizona. Tucson Arizona USA

Abstract   Blood is a concentrated suspension of red blood cells (RBCs).   Motion and deformation of RBCs can be analyzed based on knowledge of their mechanical characteristics.   Models for single-file motion of RBCs in capillaries yield predictions of apparent viscosity in good agreement with experimental results for diameters up to about 8 μm.   In living microvessels, flow resistance is also strongly influenced by the presence of a ~ 1-micron layer of macromolecules bound to the inner lining of vessel walls, the endothelial surface layer.   Two-dimensional simulations, in which each RBC is represented as a set of interconnected viscoelastic elements, predict that off-center RBCs take asymmetric shapes and drift toward the center-line. Predicted trajectories agree closely with observations in microvessels of the rat mesentery.   Realistic simulation of multiple interacting RBCs in microvessels remains as a major challenge for future work.

Keywords: Blood Flow, Capillary, Microcirculation, Red Blood Cell

1. Introduction

The microvessels, with diameters as small as 4 μm, are the terminal branches of the circulatory system.   Blood is a concentrated suspension, containing 40-45% by volume of red blood cells (erythrocytes) suspended in plasma.   The unstressed shape of a normal human RBC is a biconcave disc with a diameter of 8 microns and a thickness of 2 microns.   The interior of the cell is a concentrated haemoglobin solution, which behaves as an incompressible viscous fluid. The cell membrane has a small bending resistance, a large resistance to area change and a viscoelastic response to in-plane deformation.   RBCs undergo large deformations in passing through microvessels.   Even so, the resistance to blood flow measured in capillary-sized glass tubes is less than would be expected based on the viscosity of blood measured in bulk.

Two early theoretical analyses of RBC motion in capillaries appeared in the late 1960s (Barnard et al., 1968; Lighthill, 1968). In these analyses, cell shapes were considered to have axial symmetry.   As shown in Fig. 1, RBCs do in fact assume approximately axisymmetric shap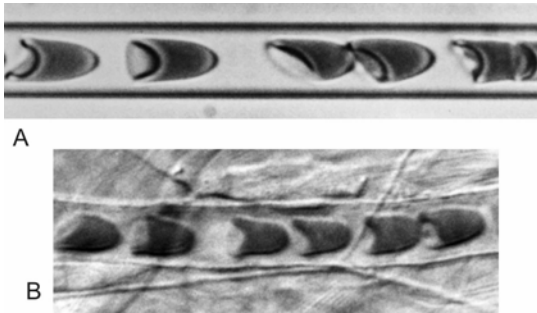es in capillaries.   Lubrication theory was used to describe the motion of the suspending fluid (plasma) in the spaces between the RBCs and the capillary walls. Analyses based on these assumptions, as discussed below, have successfully predicted the resistance to blood flow in glass tubes with capillary dimensions.

Experimental observations of blood flow in capillary networks showed much higher flow resistance than expected based on observations using glass tubes.   The main reason for this discrepancy is the presence of a layer of macromolecules lining the vessel walls. Recent studies, reviewed below, have provided insights into the physical properties of this layer and its effects on RBC motion in capillaries.

2. Apparent blood viscosity in microvessels

For steady laminar flow of a Newtonian fluid in a cylindrical tube, the volume flow rate Q is related to the driving pressure Δp according to Poiseuille's Law:

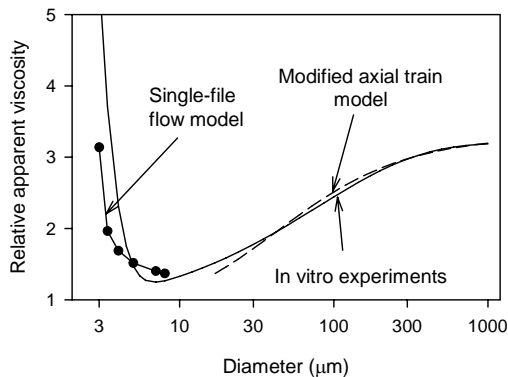$$Q = \frac{\pi}{128} \frac{\Delta p\, D^4}{L\mu} \qquad (1)$$

Fig. 1. A. Human RBCs flowing in a glass tube with diameter 7 μm. B. Blood flow through a capillary in the rat mesentery with diameter approximately 7 μm. Flow is from left to right in each case.

where L is the tube length, D is the diameter and μ is the fluid viscosity. For blood flowing in microvessels, it is convenient to define the apparent viscosity as:

$$\mu_{app} = \frac{\pi}{128} \frac{\Delta p \, D^4}{L Q} \tag{2}$$

and the relative apparent viscosity as $\mu_{rel} = \mu_{app}/\mu_p$, where μ_p is the viscosity of the plasma or other suspending fluid.

Fig. 2. Fåhraeus-Lindqvist effect in glass tubes. Solid curve: empirical fit to experimental data (Pries et al., 1992). Dots: theoretical predictions (Secomb, 1987). Dashed curve: axial-train model (see text for explanation).

Experimental data on the apparent viscosity of blood flowing in narrow glass tubes were compiled by Pries et al. (1992) and the results are shown in Fig. 2 as an empirical curve. The apparent viscosity shows a striking decrease as the tube diameter is reduced from

1 mm, a phenomenon known as the Fåhraeus-Lindqvist effect (Fåhraeus and Lindqvist, 1931).

The basic cause of this phenomenon is the tendency of flowing RBCs to migrate away from the vessel wall, creating a layer of plasma surrounding a column of flowing cells (Goldsmith et al., 1989). A simple two-phase 'axial-train' model of blood flow (Secomb, 1995) can be used to illustrate the effect of such a layer on apparent viscosity. In this model, a cylindrical central 'core' region containing RBCs, assumed to have viscosity μ_c, is surrounded by a layer of plasma with viscosity μ_p, where $\mu_c > \mu_p$. The apparent viscosity can then be calculated as

$$\mu_{rel} = \frac{1}{1 - \lambda^4 (1 - \mu_p / \mu_c)} \tag{3}$$

where λ is the ratio of the radius of the core region to the tube radius, i.e., $\lambda = 1 - h/r$ where h is the width of the cell-free plasma layer and r is the tube radius. As h increases, λ decreases from 1. Because of its fourth-power dependence on λ, the factor $1 - \lambda^4$ increases strongly with decreasing λ, and apparent viscosity declines from the core value. A relatively narrow plasma layer can have a substantial impact on apparent viscosity, because it decreases the local viscosity in the region near the wall where viscous energy dissipation would otherwise be concentrated.

3. Mechanical properties of RBCs

The mechanical properties of human RBCs have been studied extensively (Skalak, 1976; Hochmuth and Waugh, 1987). The interior of the cell behaves as a viscous incompressible fluid. The cell membrane consists of a lipid bilayer and a cytoskeleton which consists of a network of protein molecules. The membrane strongly resists area changes, and its elastic modulus of isotropic dilation is ~500 dyn/cm, whereas its modulus of shear deformation is about 0.006 dyn/cm. The lipid molecules that comprise the lipid bilayer can slide past each other relatively easily, but resist being pulled

apart. The cell membrane has a relatively small bending modulus, about 1.8×10^{-12} dyn·cm (Evans, 1983). The membrane also possesses a viscous resistance to transient in-plane shear deformations. The viscoelastic behaviour of the membrane in shear can be represented by a Kelvin solid model. According to this model, the total shear stress is represented as the sum of viscous and elastic contributions (Evans and Hochmuth, 1976), where the viscous component arises from the fluid-like behaviour of the lipid bilayer, and the elastic component arises from the stretching of the cytoskeleton.
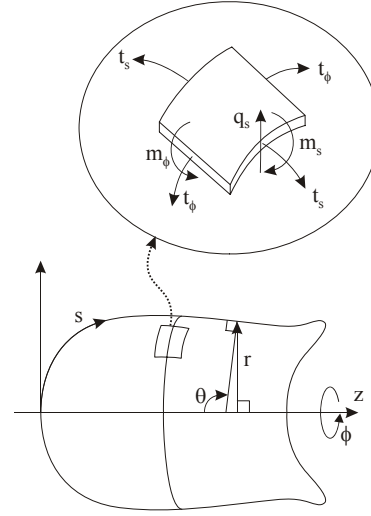
4. RBC motion in capillaries

Axisymmetric cell shapes can be described in terms of $r(s)$, distance from the axis, and $\theta(s)$, angle between the normal to the membrane and the axis, where (r, θ, φ) are cylindrical polar coordinates and s is arc length, measured from the nose of the cell (Figure 3). Membrane strain is conveniently expressed in terms of stretch ratios or extensions $\lambda_s = ds/ds_0$ and $\lambda_\varphi = r/r_0$ relative to the unstressed shape. Subscript s denotes components in a plane containing the axis, and φ denotes azimuthal components. Subscript 0 denotes corresponding values for the same material element in the unstressed state. The components of in-plane membrane curvature are $k_s(s)$ and $k_\varphi(s)$, the bending moments are $m_s(s)$ and $m_\varphi(s)$, and the components of membrane tension are $t_s(s)$ and $t_\varphi(s)$. The shear force per unit length is $q_s(s)$.

The stresses in the membrane can be evaluated using constitutive relations proposed by Evans and Skalak (1980). The bending moment is assumed to be isotropic and proportional to the increase in total curvature of the surface:

$$m_s(s) = m_\varphi(s) = B[(k_s(s) + k_\varphi(s)) - (k_s + k_\varphi)_0] \quad (4)$$

where $B = 1.8 \times 10^{-12}$ dyn·cm is the bending modulus. Viscous resistance to membrane bending is assumed to be negligible. The membrane tensions can be represented in

Fig. 3. Variables describing geometry and stress resultants in an axisymmetric shell.

terms of mean (isotropic) and deviatoric (shear) components:

$$t_s = t_m + t_d \quad \text{and} \quad t_\varphi = t_m - t_d \quad (5)$$

The membrane is nearly incompressible in a two-dimensional sense, so the deformation is locally area preserving, i.e., $\lambda_s \lambda_\varphi = 1$. A consequence of this assumption is that the mean tension, t_m, cannot be expressed in terms of membrane deformation. It depends on the forces acting on the membrane and is analogous to the hydrostatic pressure in incompressible fluid flow. The deviatoric component is

$$t_d = \frac{\mu_m}{\lambda_s} \frac{d\lambda_s}{dt} + \frac{\kappa}{2}(\lambda_s{}^2 - \lambda_\varphi{}^2) - \frac{m_s}{2}(k_s - k_\varphi) \quad (6)$$

The first term represents the viscous component of the membrane shear stress, and μ_m is the membrane shear viscosity, about 0.001 dyn·cm (Hochmuth and Waugh, 1987). The second term is the elastic component of membrane shear stress (Evans and Skalak, 1980), where $\kappa = 0.006$ dyn/cm is the shear modulus of the membrane. These two terms represent the membrane's viscoelastic behaviour in transient shear deformations as a

Kelvin solid model (Evans and Hochmuth, 1976). The third term was not included in the equations proposed by Evans and Skalak (1980), but is implicit in the assumptions of their model (Secomb, 1988).

The equations for equilibrium of normal stress, tangential stress and bending moments for an axisymmetric shell are (Timoshenko, 1940):

$$\frac{1}{r}\frac{d(rq_s)}{ds} = p + k_s t_s + k_\varphi t_\varphi \tag{7}$$

$$\frac{1}{r}\frac{d(rt_s)}{ds} = t_\varphi \frac{\cos\theta}{r} - k_s q_s - \tau \tag{8}$$

$$\frac{1}{r}\frac{d(rm_s)}{ds} = m_\varphi \frac{\cos\theta}{r} + q_s \tag{9}$$

where p is the hydrostatic pressure difference across the membrane (external minus internal) and τ is the fluid shear stress acting on the membrane produced by the motion of the external fluid. These forces can be calculated using lubrication theory to describe the motion of the fluid around the cell. According to the assumptions of lubrication theory, the pressure is $p(z)$ and the axial velocity $u(\sigma, z)$ of fluid in the gap satisfies

$$\frac{\mu_p}{\sigma}\frac{\partial}{\partial\sigma}\left(\sigma\frac{\partial u}{\partial\sigma}\right) = \frac{dp}{dz} \tag{10}$$

in cylindrical coordinates (σ, φ, z) moving with the cell, where μ_p is the fluid viscosity. Also, $u = 0$ on the cell surface, $\sigma = r(z)$, and $u = u_0$ at the wall, $\sigma = a$ where $-u_0$ is the cell velocity and a is the vessel radius. The 'leakback,' i.e., the volume flow rate of fluid relative to the cell per unit circumference, is given by

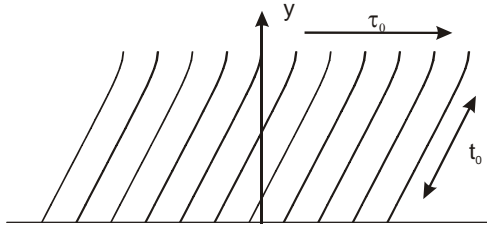$$q_0 = \int_r^a u(\sigma, z)\frac{\sigma}{a}d\sigma \tag{11}$$

Since the suspending fluid is incompressible, q_0 is independent of z. These equations can be solved for the pressure gradient and shear stress acting on the cell surface, in terms of $r(z)$ and q_0, and a system of ordinary differential equations can be derived for the variables describing cell shape and membrane stresses. These equations can be solved numerically to predict steady-state RBC shapes under a variety of conditions (Secomb et al., 1986). Good agreement is found between predicted cell shapes and apparent viscosity and corresponding experimental observations (Secomb et al., 1986; Secomb, 1987, 1991, 2003).

5. The endothelial surface layer

Based on observations of blood flow velocities in microvascular networks of the rat mesentery, Pries et al. (1990, 1994) deduced an empirical equation for blood viscosity in vivo as a function of vessel diameter and hematocrit. This equation predicts higher values of apparent viscosity in capillaries than was observed in glass tubes with corresponding diameters. The main cause of this difference was found to be the presence of a layer of bound or adsorbed macromolecules, known as the endothelial surface layer (ESL), lining the interior surfaces of blood vessels. This layer is about 1 μm in thickness, and is capable of impeding plasma flow and excluding RBCs. The ability of the ESL to impede plasma flow implies that it has a hydraulic resistivity of at least 10^8 dyn·s/cm^4 (Secomb et al., 1998).

The physical properties of the ESL have not been definitely established. Experimental evidence indicates that it has finite resistance to compression. It is able to withstand the shear stress exerted by the flowing blood. Also, it recovers its width in about 1 s after being compressed by a passing white blood cell (Vink et al., 1999). Pries et al. (2000) hypothesized that the layer consists of an array of glycoprotein chains or strands attached to the endothelial surface (Figure 4), and that it resists flattening because of colloid osmotic pressures generated by plasma proteins adsorbed to the strands (Silberberg, 1991). According to this hypothesis, the colloid osmotic pressure within the ESL is increased by an amount $\Delta\pi_p$ above that of free plasma, and this additional pressure is balanced by tension in membrane-bound strands. To

Fig. 4. Model for ESL mechanics. A matrix of strands is attached to the endothelial cell membrane ($y = 0$). Strands have tension t_0 per unit membrane area. When a fluid shear stress τ_0 is imposed, the stress is transmitted into the matrix in the region near the tips of the strands. The deflection of the strands from the perpendicular to the membrane allows the matrix to support the shear stress.

compress the ESL, an applied force must exceed $\Delta\pi_p$. The fluid shear stress acting on the ESL is transferred to this matrix. Transmission of shear stress to endothelial cells therefore occurs almost entirely via the attachment points of the ESL to the cell membrane (Secomb et al., 2001). Other properties of the ESL have been reviewed elsewhere (Pries et al., 2000).

Mechanical interactions between the ESL and RBCs have been analyzed in several theoretical studies. Damiano (1998) and Secomb et al. (1998) modelled the motion of flexible RBCs through a capillary lined with an ESL, and predicted the effects of the layer on relative apparent viscosity and on the ratio of tube to discharge hematocrit. Feng and Weinbaum (2000) showed that motion of red cells past the ESL generates a fluid mechanical "lift" force that can cause the cells to glide over the layer. This provides an explanation for the observation (Vink and Duling, 1996) that stationary red cells expand to fill the entire capillary, even though flowing cells are excluded from the layer.
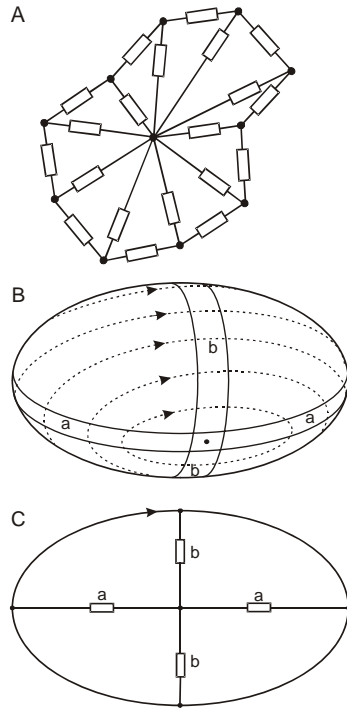
In reality, capillaries do not have uniform cylindrical shapes. Projecting endothelial cell nuclei and other irregularities cause the cross-section to vary with position along the capillary. Secomb et al. (2002) examined the effects of ESL on the motion and deformation of RBCs flowing along non-uniform

capillaries. In this case, a time-dependent formulation of the equations of lubrication theory was used to predict the dynamic variation in RBC shape as it encounters sinusoidal variations in capillary diameter. The peak shear stresses acting on the RBC membrane as the cell traverses a local narrowing were also calculated. It was found that the ESL buffers RBCs from transient deformations and high levels of shear stress experienced during their transit through the irregularities of the microcirculation. The average lifetime of a human RBC is around 120 days, and during that time it makes about 3×10^5 transits through the circulatory system. Mechanical flexing of cells is one of the factors that limits their lifetimes (Kameneva et al., 1995). Therefore, the endothelial surface layer may preserve RBCs from flow-induced damage as they traverse capillaries.

6. Two-dimensional RBC model

Several aspects of RBC motion in microvessels cannot be well described by axisymmetric models. For such cases, we developed a two-dimensional approach in which the cross-sectional shape of each RBC is represented by an assemblage of viscoelastic elements on the perimeter and in the interior of the cell (Figure 5A) (Secomb et al., 2007). The internal elements represent both the internal viscosity of the cell and the cell membrane's resistance to three-dimensional out-of-plane deformations. Membrane bending elasticity is represented by an elastic resistance at the nodes.
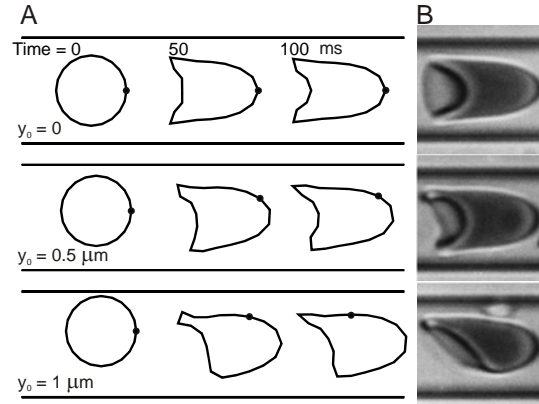
When placed in simple shear flow of high-viscosity fluid, RBCs exhibit stable orientations and cyclic 'tank-treading' motion of the membrane around the cell interior. In this motion, a band of membrane around the cell is alternately lengthened and shortened (Figure 5B). This continuous deformation results in viscous energy dissipation in the membrane. The internal viscous elements represent resistance to this motion. The parameters of the model were determined by matching model behaviour to observations of tank-treading.

Fig. 5. A. Two-dimensional model for RBC. Rectangles represent viscoelastic elements. B, C. Relationship between internal viscous elements and membrane deformation in tank-treading. Bands of membrane (a,b) alternately shorten and elongate during tank-treading.

The fluid flow around the model cell results in loadings on the external elements. The longitudinal (tension) force $t_i(s)$, the transverse (shear) force $q_i(s)$ and the bending moment $m_i(s)$ acting in external element i are consequently functions of distance s along the element. The equations of mechanical equilibrium for this system are given by Secomb et al. (2007). RBCs deform at effectively constant volume. This property is represented by assigning an internal pressure that depends on the cell area. The suspending medium is a viscous incompressible fluid, in Stokes flow. A finite element package (FlexPDE, PDE Solutions Inc., Antioch, CA) was used to solve the resulting system of coupled equations. When a cell closely approaches the domain boundary, the

mesh generator controls the aspect ratio of the elements, so that a large number of small elements are used. The initial shape was assumed to be circular, so as not to bias the subsequent evolution of cell shape.
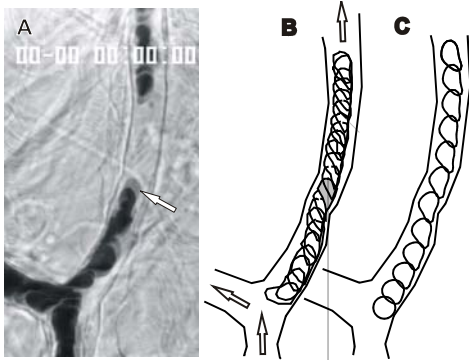

Fig. 6. Predicted motion and deformation of cells in an 8-μm channel. Flow rate is adjusted so that cell velocity is approximately 1.25 mm/s. Results are presented for cells with initial displacements 0, 0.5, 1 μm from the centre-line. A. Predicted cell shapes initially and after 50 and 100 ms. Dot on cell outline represents a node fixed in the cell. B. Observed human RBC shapes in a single glass capillary with diameter 7 μm. Three cells are shown with varying orientations and degrees of asymmetry.
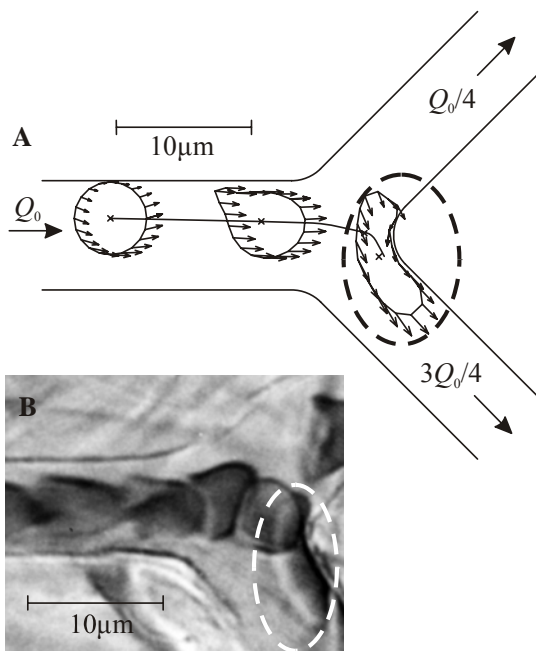
In Figure 6, predictions for a single cell flowing along an 8-μm channel (A) are compared with experimental observations in glass tubes (B). Good qualitative agreement with observed shapes is seen.

Trajectories and shapes of RBCs computed by this method agree well with observations of red cell motions in living tissues (Figure 7). Results are shown in Figure 8A for a RBC in a bifurcation. In this example, the cell starts near the upper boundary, and migrates toward the centerline in the upstream channel. It impinges on the flow divider, and conforms to its contour, forming a 'sandbag' shape. This shape is similar to observed shapes in bifurcations (Figure 8B). As indicated by the velocity vectors, this cell eventually enters the lower branch, which has the higher flow rate.

Fig. 7. Observations and simulations of RBC motion in rat mesenteric microvessels. A. Microvessels selected for observation. Arrow: RBC whose motion was tracked. B. Superimposed digitized outlines of vessel wall and of selected isolated cells in successive video frames at 10-ms intervals. Arrows show flow directions. C. Predicted cell shapes at 20-ms intervals. From Secomb et al. (2007).

Fig. 8. Predicted motion and deformation of a cell in a bifurcation. Flow rate = 8 μm^2/ms. A Cell shapes at t = 0, 10, and 30 ms. Solid line: center-of-mass trajectory. B Photomicrograph of red blood cells in a bifurcation (courtesy of Dr. A.R. Pries). Cell outlined with an ellipse is similar in shape to that indicated in A. From Barber et al. (2008).

7. Discussion

Substantial progress has been made in understanding the mechanics of individual RBC motion in capillaries. In microvessels with diameters of 10 μm and above, multiple cells typically interact within each vessel cross-section. These interactions are important in determining apparent viscosity in this diameter range. Simulation of the motion of multiple interacting RBCs with realistic mechanical properties remains a difficult computational challenge, but is needed in order to fully understand the flow behaviour of blood in the microcirculation.

Acknowledgements

References

Barber, J.O., Alberding, J.P., Restrepo, J.M., Secomb, T.W., 2008. Simulated two-dimensional red blood cell motion, deformation, and partitioning in microvessel bifurcations. Ann. Biomed. Eng 36:1690-1698.

Barnard, A.C.L., Lopez, L., Hellums, J.D., 1968. Basic theory of blood flow in capillaries. Microvasc. Res. 1:23-34.

Damiano, E.R., 1998. The effect of the endothelial-cell glycocalyx on the motion of red blood cells through capillaries. Microvasc. Res. 55:77-91.

Evans, E.A., 1983. Bending elastic modulus of red blood cell membrane derived from buckling instability in micropipet aspiration tests. Biophys. J. 43:27-30.

Evans, E.A., Hochmuth, R.M., 1976. Membrane viscoelasticity. Biophys. J. 16:1-11.

Evans, E.A. and Skalak, R., 1980. Mechanics and Thermodynamics of Biomembranes. CRC Press, Boca Raton, Florida.

Fahraeus, R., Lindqvist, T., 1931. The viscosity of the blood in narrow capillary tubes. Am. J. Physiol. 96:562-568.

Feng, J., Weinbaum, S., 2000. Lubrication theory in highly compressible porous media: the mechanics of skiing, from red cells to humans. Journal of Fluid Mechanics 422:281-317.

Goldsmith, H.L., Cokelet, G.R., Gaehtgens, P., 1989. Robin Fahraeus: evolution of his concepts in cardiovascular physiology. Am. J. Physiol 257:H1005-H1015.

Hochmuth, R.M., Waugh, R.E., 1987. Erythrocyte membrane elasticity and viscosity. Annu. Rev. Physiol 49:209-219.

Kameneva, M.V., Antaki, J.F., Borovetz, H.S., Griffith, B.P., Butler, K.C., Yeleswarapu, K.K., Watach, M.J., Kormos, R.L., 1995. Mechanisms of red blood cell trauma in assisted circulation. Rheologic similarities of red blood cell transformations due to natural aging and mechanical stress. ASAIO J. 41:M457-M460.

Lighthill, M.J., 1968. Pressure-forcing of tightly fitting pellets along fluid-filled elastic tubes. Journal of Fluid Mechanics 34:113-143.

Pries, A.R., Neuhaus, D., Gaehtgens, P., 1992. Blood viscosity in tube flow: dependence on diameter and hematocrit. Am. J. Physiol. 263:H1770-H1778.

Pries, A.R., Secomb, T.W., Gaehtgens, P., 2000. The endothelial surface layer. Pflugers Arch. 440:653-666.

Pries, A.R., Secomb, T.W., Gaehtgens, P., Gross, J.F., 1990. Blood flow in microvascular networks. Experiments and simulation. Circ. Res. 67:826-834.

Pries, A.R., Secomb, T.W., Gessner, T., Sperandio, M.B., Gross, J.F., Gaehtgens, P., 1994. Resistance to blood flow in microvessels in vivo. Circ. Res. 75:904-915.

Secomb, T.W., 1987. Flow-dependent rheological properties of blood in capillaries. Microvasc. Res. 34:46-58.

Secomb, T.W., 1988. Interaction between bending and tension forces in bilayer membranes. Biophys. J. 54:743-746.

Secomb, T.W., 1991. Red blood cell mechanics and capillary blood rheology. Cell Biophys. 18:231-251.

Secomb, T.W., 1995. Mechanics of blood flow in the microcirculation. Symp. Soc. Exp. Biol. 49:305-321.

Secomb, T.W., 2003. Mechanics of red blood cells and blood flow in narrow tubes. *In* Hydrodynamics of Capsules and Cells. C.

Pozrikidis, editor. Chapman & Hall/CRC, Boca Raton, Florida. 163-96.

Secomb, T.W., Hsu, R., Pries, A.R., 1998. A model for red blood cell motion in glycocalyx-lined capillaries. Am. J. Physiol 274:H1016-H1022.

Secomb, T.W., Hsu, R., Pries, A.R., 2001. Effect of the endothelial surface layer on transmission of fluid shear stress to endothelial cells. Biorheology 38:143-150.

Secomb, T.W., Hsu, R., Pries, A.R., 2002. Blood flow and red blood cell deformation in nonuniform capillaries: effects of the endothelial surface layer. Microcirculation 9:189-196.

Secomb, T.W., Skalak, R., Ozkaya, N., Gross, J.F., 1986. Flow of axisymmetric red blood cells in narrow capillaries. Journal of Fluid Mechanics 163:405-423.

Secomb, T.W., Styp-Rekowska, B., Pries, A.R., 2007. Two-dimensional simulation of red blood cell deformation and lateral migration in microvessels. Ann. Biomed. Eng 35:755-765.

Silberberg, A., 1991. Polyelectrolytes at the Endothelial-Cell Surface. Biophysical Chemistry 41:9-13.

Skalak, R., 1976. Rheology of red blood cell membrane. *In* Microcirculation, Vol. I. J. Grayson and W. Zingg, editors. New York. 53-70.

Timoshenko, S. 1940. Theory of Plates and Shells. McGraw-Hill, New York.

Vink, H., Duling, B.R., 1996. Identification of distinct luminal domains for macromolecules, erythrocytes, and leukocytes within mammalian capillaries. Circ. Res. 79:581-589.

Vink, H., Duling, B.R., Spaan, J.A.E., 1999. Mechanical properties of the endothelial surface layer. FASEB Journal 13:A11.